ELSEVIER

Polymer 41 (2000) 4889–4900

polymer

Thermal behaviour and morphology of homogeneous ethylene–1-octene copolymers with high comonomer contents

S. Vanden Eynde[a], V.B.F. Mathot[a,*], M.H.J. Koch[b], H. Reynaers[a]

[a]*Departement Scheikunde, Laboratorium voor Macromoleculaire Structuurchemie, Katholieke Universiteit Leuven, Celestijnenlaan 200F, B-3001 Heverlee, Belgium*

[b]*European Molecular Biology Laboratory, EMBL c/o DESY, Notkestraße 85, D-22603 Hamburg, Germany*

Received 21 July 1999; accepted 29 September 1999

Abstract

The thermal behaviour and morphology of a series of homogeneous ethylene–1-octene copolymers, covering a wide range of 1-octene content up to 44 mole%, is studied using differential scanning calorimetry (DSC), time-resolved small-angle X-ray scattering (SAXS) and wide-angle X-ray diffraction (WAXD). The influence of the comonomer (1-octene) content, as well as the influence of the comonomer type (branch length) are investigated by comparison with previous results on homogeneous ethylene–propylene and ethylene–1-butene copolymers. Special emphasis is put on copolymers with high comonomer contents or low densities (<870 kg/m^3) at room temperature. The thermal behaviour and the morphology of the present copolymers reveal no discontinuities with increasing comonomer content and support a model in which the morphology changes gradually from a lamellar base morphology into a granular one consisting of small blocky structures and, possibly via fringed-micelles, into a morphology consisting of loosely packed ethylene sequences. The latter structures are too small and/or too imperfect to be detected by WAXD. However, SAXS and DSC are sensitive to them and are useful techniques over the whole comonomer content range.

Keywords: Crystallisation; Differential scanning calorimetry; Homogeneous ethylene–1-octene copolymers

1. Introduction

Polyolefines play an important role in research, development and applications of polymers [1–4]. Each of their daily life applications relies on a unique combination of molecular structure (chain microstructure) and processing. To control and influence the final properties of polymers, a good knowledge of the relations between the chain microstructure, which is determined by the synthetic step, the crystallisation conditions, the morphology and the resulting properties is important.

Beside copolymers like LLDPEs and VLDPEs [3,5], which are *heterogeneous* with respect to the intermolecular distribution of the side chain branches, homogeneous copolymers are of growing interest because of recent developments in single-site metallocene catalysis [6–8] and because of their potential applications, e.g. use as impact modifier, in food packaging, etc. Copolymers, like the ethylene–1-octene (EO) copolymers investigated here, are called *homogeneous* [3], when the comonomer addition during polymerisation can be described by a single set of chain propagation probabilities (P-set). All chains are characterised by the same comonomer/monomer ratio and there are no statistical differences within and between the molecules.

Beside the comonomer content, the comonomer type, or side branch length, also has an important influence on the thermal behaviour and morphology of copolymers, because the length of the short chain branches determines whether or not they are inserted in the crystal lattice. Methyl branches can be incorporated at interstitial positions [9–11] leading to crystal defects, while the longer hexyl branches are excluded from the crystal core. Longer branches are also not incorporated, but the side chain branches may still crystallise [12,13].

The SAXS and WAXD measurements were performed simultaneously in real-time using synchrotron radiation. The results on homogeneous EO copolymers with relatively low comonomer contents (JW 1114, JW 1116, JW 1120 and JW 1121), including linear correlation function analysis were discussed by Peeters et al. [14,15]. Linear correlation functions [16] were not calculated for the copolymers with high 1-octene contents, as reported here, because of the

* Corresponding author.
E-mail address: vincent.mathot@chem.kuleuven.ac.be (V.B.F. Mathot).

0032-3861/00/$ - see front matter
PII: S0032-3861(99)00712-0

Table 1
Molecular characteristics of the LPE-sample and the homogeneous etheylene–1-octene copolymers (n.d. = not determined)

Sample	Mole% 1-Octene	$D^{23°C}$ (kg/m^3)	$[\eta]^{135}_{dec}$ (dl/g)	M_n^* (kg/mol)	M_w^* (kg/mol)	M_z^* (kg/mol)
JW 1114(LPE)	0.0	n.d.		20	52	99
JW 1116	2.1	n.d.		21	47	87
JW 1120	5.2	n.d.		16	31	53
JW 1121	8.0	n.d.		17	34	48
EO J (= EO V)	11.5	872	3.04	110	215	350
EO I	14.2	860	2.81	94	190	320
EO H	20.8	853	1.44	47	97	160
EO D	24.0	n.d.	0.95	27	58	93
EO E	26.3	n.d.	0.53	n.d.	n.d.	n.d.
EO F	27.5	n.d.	0.52	n.d.	n.d.	n.d.
EO C	31.1	n.d.	0.59	n.d.	n.d.	n.d.
EO A	44.0	n.d.	0.31	8	16	26

absence of clear lamellar structures and only the SAXS-invariants were used for interpretation. X-ray diffraction and thermal analysis and calorimetry (DSC) provide a powerful combination for the investigation of the crystallisation and melting behaviour and morphology of the present materials. To facilitate comparison, the EO copolymers were submitted to measurements similar to those performed earlier on homogeneous ethylene–propylene (EP) and ethylene–1-butene (EB) copolymers [17].

2. Experimental

2.1. Samples

The homogeneous EO copolymers were synthesised using a homogeneous vanadium-based catalyst [14–16,18] which was also used for the previous EP copolymer series [17]. A linear polyethylene (LPE) sample, JW1114, was also studied and used as a reference material. The comonomer content, covering a wide range from 2.1 mole% up to 44 mole% 1-octene, was controlled by varying the 1-octene/ethylene ratio. Table 1 gives an overview of the molecular characteristics of the investigated LPE-sample and the homogeneous EO copolymers. The (apparent) weight and number molar masses were determined by size exclusion chromatography (SEC) in 1,2,4-trichlorobenzene at 135 or 150°C using universal (indicated by *) calibrations. ^{13}C-NMR was used to determine the comonomer content. The density measurements were performed at room temperature after compression moulding of the samples.

2.2. Techniques and methods

2.2.1. DSC

The calorimetric measurements were carried out using a TA Instruments 2920 DSC in helium atmosphere with a pulsed nitrogen cooling system. Pure indium and benzophenone were used for temperature calibration. The sample masses varied from 5 to 20 mg (±0.02 mg) with increasing comonomer content. The (co)polymer was held for 5 min in the melt (at 200°C for the JW-coded copolymers and at 150°C for the EO-coded copolymers) to erase previous history, and subsequently cooled to −90°C at −10°C/min. After 5 min at −90°C, the sample was heated at the same rate. An empty pan measurement was subtracted from each DSC run.

Because of the flat and broad DSC-curves, especially in the case of copolymers with the highest comonomer contents, the identification of the crystallisation (T_c) and melting (T_m) temperatures with the maximum in the cooling and heating curves, respectively (T_x^{peak}) alone is not sufficiently indicative. Therefore, T_c and T_m of the copolymers were also defined in two other ways: (1) the temperature at which the extrapolation from the melt and the extrapolation from the peak shoulder at the high temperature side cross (T_x^{eo}, extrapolated on/offset); and (2) the temperature at which the DSC-signal deviates from the extrapolation from the melt at the high temperature side (T_x^{ro}, real on/offset). The glass transition temperature (T_g) was calculated using the enthalpy method [19–21].

The mass fraction crystallinity as a function of temperature, $w^c(T)$, was calculated after Mathot et al. [22,23] using a linear extrapolation from the melt as a good approximation of the heat flow of the fully amorphous phase. The following equation was used:

$$w^c(T) = \frac{(A_1 - A_2)_T}{h_a(T) - h_c(T)} \quad (1)$$

where A_1 and A_2 are the areas enclosed above and below the line obtained by linear extrapolation from the melt respectively, and the measured curve. Eq. (1) is derived from Eq. (2), which results from the additivity of the enthalpies of the crystalline and amorphous phases [3]

$$w^c(T) = \frac{h_a(T) - h(T)}{h_a(T) - h_c(T)} \quad (2)$$

The LPE reference values were taken from literature [24]. The heat capacity values of the amorphous phase, $c_{pa}(T)$, for LPE [24], which are based on Eq. (10) in Wunderlich et al. [25], were used at temperatures above 17°C, as for LPE.

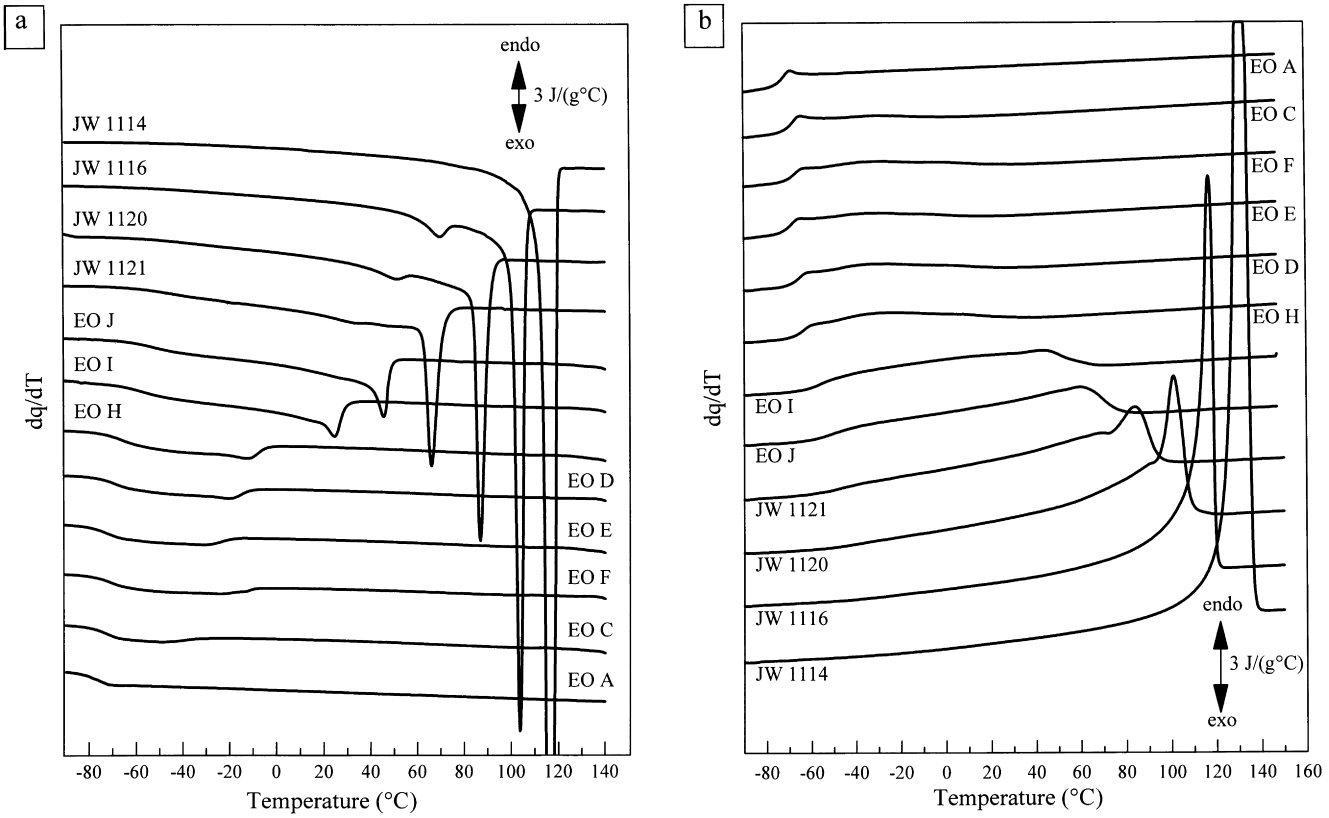

Fig. 1. Cooling (a) and heating (b) curves of JW 1114 and homogeneous ethylene–1-octene copolymers; rate 10°C/min. The curves have been displaced along the ordinate for better visualisation.

Because, contrary to LPE, the copolymers show abrupt glass transitions, the gradually changing $c_{pa}(T)$ in case of LPE below 17°C was replaced by continuation of Eq. (10).

2.3. Time-resolved SAXS/WAXD

Simultaneous SAXS and WAXD measurements were performed in real-time on the X33 double focusing camera of the EMBL in HASYLAB, at the storage ring DORIS III of the Deutsches Elektronen Synchrotron (DESY, Hamburg) at a wavelength of 1.5 Å [26]. The camera was equipped with proportional gas detectors with delay line readout [27]. Dry calcified turkey tendon collagen was used for the calibration of the scattering vector $s = 2 \sin \theta/\lambda$, with 2θ the scattering angle and λ the wavelength. In the WAXD region 2θ was calibrated using the 110- and 200-reflections of quenched JW 1114 (LPE) at 50°C, previously recorded at the same temperature on a Rigaku high-temperature X-ray diffractometer which was calibrated with a silicon standard [28].

The low-density EO copolymer samples (about 1 mm thick) were first held for 5 min in the melt at 150°C, then cooled at −5°C/min to −60°C and subsequently heated into the melt at 10°C/min using a Mettler FP-82HT hot stage, mounted perpendicularly to the incident X-ray beam. Pulsed nitrogen was used to control the cooling of the hot stage down to −60°C. The oven was calibrated using the melting point of benzoic acid ($T_m = 122$°C).

The SAXS and WAXD intensities were normalised to the intensity of the primary beam. After correction for the detector response, an averaged melt pattern was subtracted from each SAXS pattern as a background correction.

The SAXS-invariant, $Q(T)$, or total scattering power of the system, was calculated by integration of the scattering intensity $I(s, T)$ with respect to s:

$$Q(T) = \int_0^\infty I(s, T)s^2 \, ds \tag{3}$$

Because data were not collected from zero to infinity, but over a limited s-range, the presented calculations lead to an approximation of Q which, however, as shown in some previous papers, still yields all the correct trends.

For an ideal two-phase system the invariant can be written as:

$$Q_{id}(T) = C\alpha_s\phi_L(T)(1\text{-}\phi_L(T))[d_c(T) - d_a(T)]^2 \tag{4}$$

where C is a constant depending on the instrument and representing the conversion factor from mass (g/cm^3) to electron density (mol e$^-$/cm^3); α_s is the fraction of semi-crystalline regions within the total irradiated sample volume [29]; $\phi_L(T)$ represents the temperature-dependent local volume fraction crystallinity in the semi-crystalline regions;

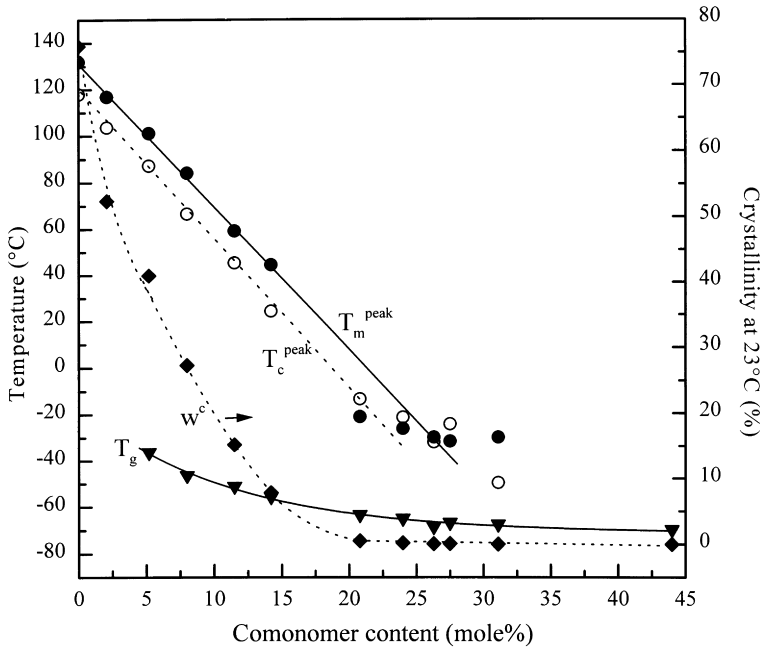

Fig. 2. Thermal characteristics of JW 1114 and EO copolymers obtained from DSC measurements during heating at 10°C/min after cooling at the same rate: T_c^{peak} (○), T_m^{peak} (●), T_g (▼); w^c at 23°C (◆, right ordinate). The lines are guides to the eye.

$d_c(T)$ and $d_a(T)$ are the temperature-dependent mass densities of the crystalline and amorphous phase, respectively.

3. Results and discussion

3.1. Influence of the comonomer content on thermal behaviour and morphology

Short chain branches in ethylene–1-alkene copolymers, which disrupt the regularity of the main chain, exert a large influence on the crystallisation and melting behaviour. The presence and the amount of branches, as well as their distribution within the main chain are determining factors for the crystallisation/melting temperature distributions, the degree of crystallinity, the density at room temperature and the temperature-dependent properties of the material [2,14,17,18,30].

Ethylene copolymers are characterised by their ethylene sequence length distribution (ESLD). During crystallisation a corresponding crystallisation temperature distribution will arise which in turn will lead to a crystallite size distribution. During heating the latter will, for thermodynamic reasons, result in a melting temperature distribution. Although nucleation plays an important role in crystallisation, the associated kinetics cannot yet be described by any theoretical model. Therefore, often the melting process is investigated and, more specifically, the relationship between the ESLD and the melting temperature distribution. However, it should be emphasised that also during melting, kinetic effects such as reorganisation by recrystallisation can occur [15,31–33], reflecting that macromolecular crystallites are often metastable. Obviously, the exact relationship between the distributions mentioned is not simple, neither for crystallisation nor for melting, which is why both melting *and* crystallisation are discussed below.

The DSC-curves of the homogeneous EO copolymers during cooling and subsequent heating are shown in Fig. 1, while in Fig. 2 some characteristics are given as a function of the comonomer content: the crystallisation and melting peak temperatures (T_c^{peak} and T_m^{peak}), the glass transition temperature (T_g) and the crystallinity at 23°C (w^c(23°C), see also Fig. 10).

The influence of increasing comonomer content on thermal behaviour is reflected in the shape, position and size of the DSC-curves and the effects being similar to those observed for the homogeneous EP and EB copolymers [17].

With increasing comonomer content, the DSC-curves during cooling and heating become flatter and broader, reflecting broad crystallite distributions. There is also a shift to lower temperatures, so that the crystallisation and melting regions approach the glass transition region at high comonomer contents. The copolymer with the largest 1-octene amount (44 mole% 1-octene), revealing no exothermic peak while the small endothermic peak is assumed to be caused by enthalpy recovery; only shows a sharp glass transition. T_c^{peak} and T_m^{peak} decrease nearly linearly with increasing comonomer content (Fig. 2). At high 1-octene contents (>20 mole%) T_x^{peak} deviates from linearity and there is a switch in the relative position of T_c^{peak} and the corresponding T_m^{peak}. The latter was also observed for ethylene copolymers with propylene contents above 30 mole% [17]. These features can be explained by the more difficult and less accurate peak determination in the

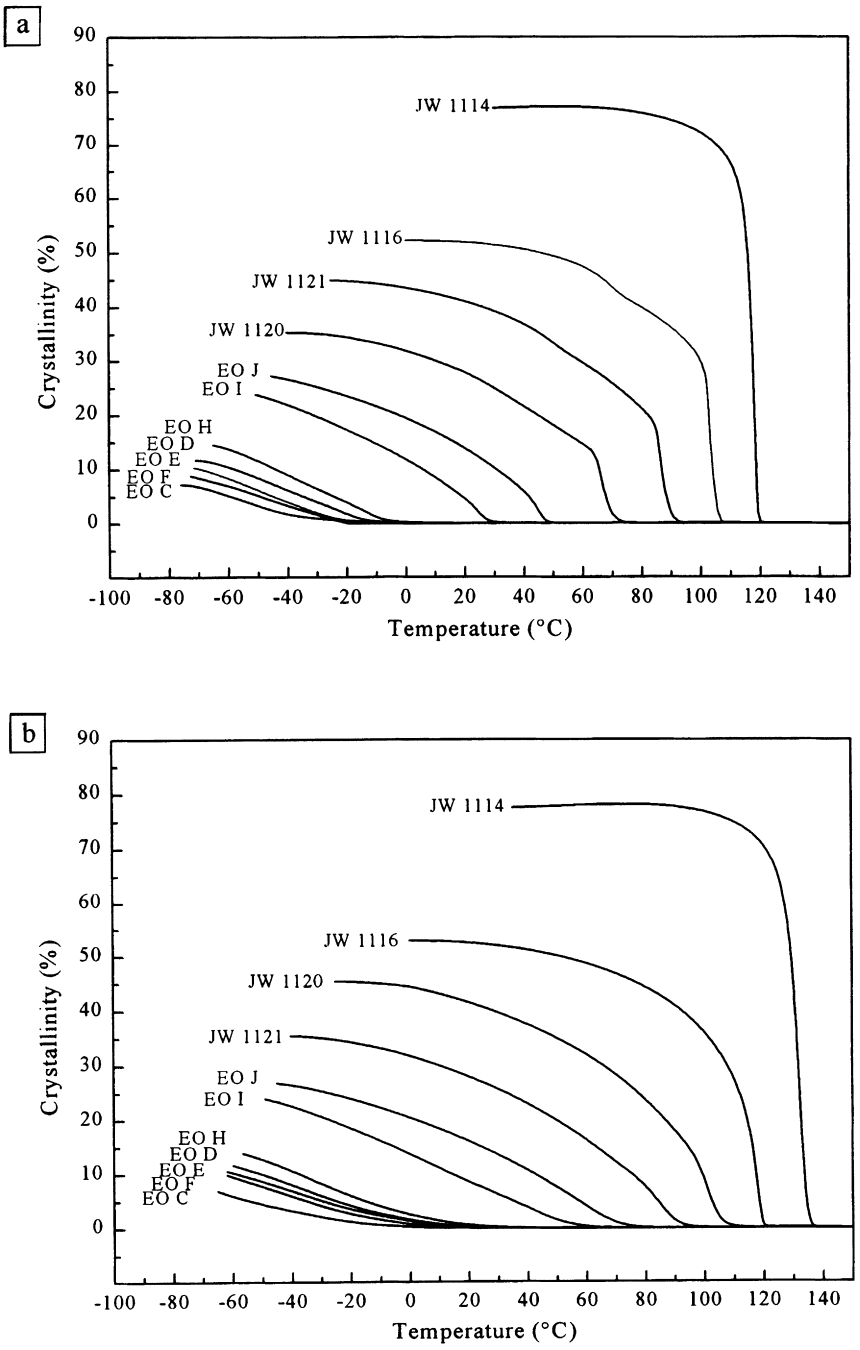

Fig. 3. Crystallinity as a function of temperature of JW 1114 and homogeneous EO copolymers, calculated from DSC curves by extrapolation from the melt, during cooling (a) and subsequent heating (b), both at 10°C/min.

very broad and flat DSC curves at high comonomer contents. The reason for the deviating behaviour of the EO F sample in Fig. 1, which has higher T_c- and T_m-values than the other samples, was not further investigated.

Beside the broadening and the shift of the DSC-curves with increasing comonomer content, the DSC-peak area also becomes smaller, corresponding to lower crystallinities.

Further, (de)vitrification takes place at lowering temperatures, while the associated stepwise change in dq/dT is more pronounced at high comonomer contents. The T_g-values decrease very slightly compared to T_c and T_m and evolve more or less towards a constant value (Fig. 2). This levelling effect can be explained by the fact that with continuing increase in comonomer content, the T_g will evolve to the T_g-value of the homopolymer poly-1-octene [34] around −65°C. It should be mentioned that, for the EO copolymers, with increasing comonomer content also the molar mass decreases, possibly causing additional lowering of T_g.

In the cooling curves of the copolymers with the lowest

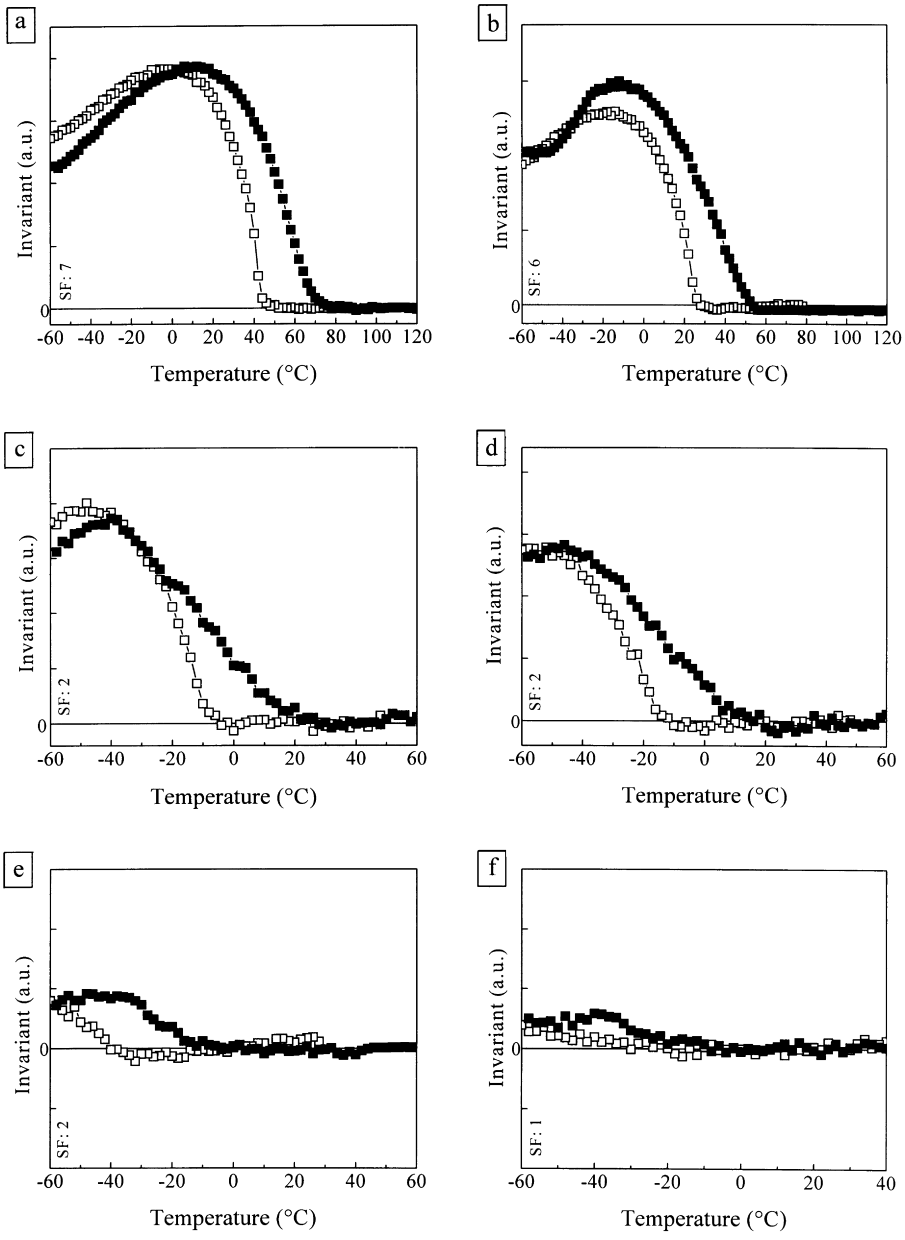

Fig. 4. SAXS invariants of homogeneous EO copolymers during cooling (□) and subsequent heating (■) at 10°C/min: (a) EO J; (b) EO I; (c) EO H; (d) EO D; (e) EO C; (f) EO A. Arbitrary invariant scale, but comparable using the scale factors (SF) given.

comonomer contents a small peak can be observed at about 35°C below the main exotherm. This small exotherm is also present in homogeneous EP and EB copolymers [17] and has been speculatively ascribed to homogeneous nucleation [3].

The comonomer content-dependent changes in the shape, the position and the size of the DSC-curves mentioned above, can be explained by the increasing amount of branches which reduces the capability of crystallisation by shortening the lengths of the crystallisable ethylene sequences. Moreover, chain mobility is decreased at low-temperature transitions, and, hence, the rate at which segments of the same length should be sorted is lower [35–37] as expected from thermodynamic considerations. Both effects result in the formation of smaller, less perfect and less stable crystallites with increasing comonomer content [1,2], as also reflected in the decreasing peak areas (lowering crystallinities). Fig. 3(a) and (b) shows the crystallinities as a function of temperature during cooling and subsequent heating, obtained from the DSC-curves shown in Fig. 1. As soon as crystallisation starts during cooling, the crystallinity increases until it reaches a maximum value just above the glass transition. The maximal crystallinities after cooling and before heating are the same, as expected for a closed cycle. The crystallinities as well as the on- and off-set temperatures of the crystallinity

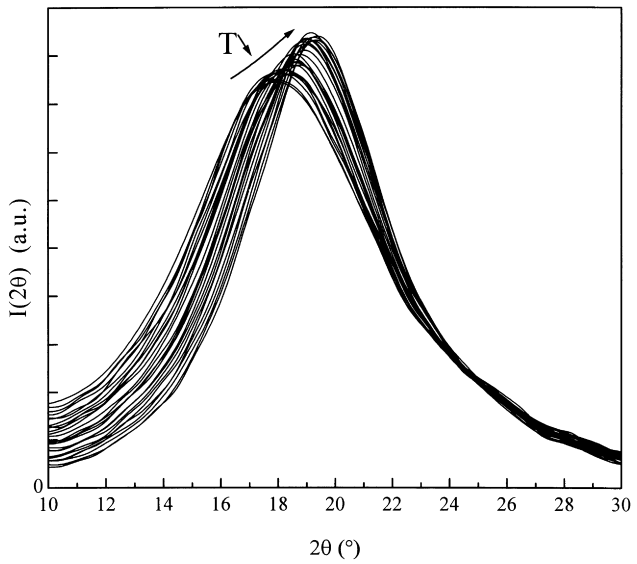

Fig. 5. WAXD-patterns of EO A during cooling from 90 to −60°C at −5°C/min.

curves of EO J are consistent with those obtained from heat capacity measurements by Mathot et al. [2].

The time-resolved SAXS curves of the low-density EO copolymers reveal a maximum for all copolymers, after subtraction of an averaged melt pattern, indicating the presence of periodic electron density fluctuations leading to a correlation maximum, whose intensity decreases with increasing comonomer content. However, this correlation maximum was not analysed, because these copolymers have no lamellar morphology and only the invariants were used for interpretation.

The invariants calculated from the SAXS data of the EO copolymers, are shown in Fig. 4. The invariants are all given in the same arbitrary units (a.u.), although they have been drawn on different scales for better visualisation. As long as the copolymer is in the melt there are no macroscopic electron density fluctuations and the invariant is close to zero (see Eq. (4)). The maxima in the invariants result from the opposed temperature dependencies of the terms $\phi_L(1-\phi_L)$ and $(d_c - d_a)^2$ at crystallinities below 50%, which is the case for the present EO copolymers. With increasing 1-octene content, the invariant sets on (cooling) and off (heating) at lower temperatures, while the scattered intensity drops because of the reduced crystallinity and the reduced electron density differences. The off/onset temperatures of the SAXS invariants are in good agreement with those of the crystallinities obtained from DSC (Fig. 3). The difference between the invariant (and crystallinity) curves during cooling and heating is due to hysteresis effects. In contrast to melting, nuclei have to be formed for crystallisation, leading to an undercooling.

One should notice that the EO A sample (44 mol 1-octene) still shows a change in the SAXS-invariant, while on the basis of DSC results the copolymer is thought to be completely amorphous, see before. This means that there are still detectable electron density fluctuations above the level of the amorphous regions. This interesting observation suggests that SAXS is even more sensitive than DSC, but real heat capacity measurements need to be done to confirm this. Moreover, the time-resolved WAXD-patterns of EO A, where absolutely no crystalline reflections are observed, become narrower/sharper and shift to higher angles during cooling from 90 to −60°C, as illustrated in Fig. 5. Opposite features are observed during heating. The narrowing of the peak during cooling suggests that the EO A sample is not completely amorphous, in the sense of liquid-like amorphous as in the melt, but that a kind of ordering develops during cooling which disappears during heating.

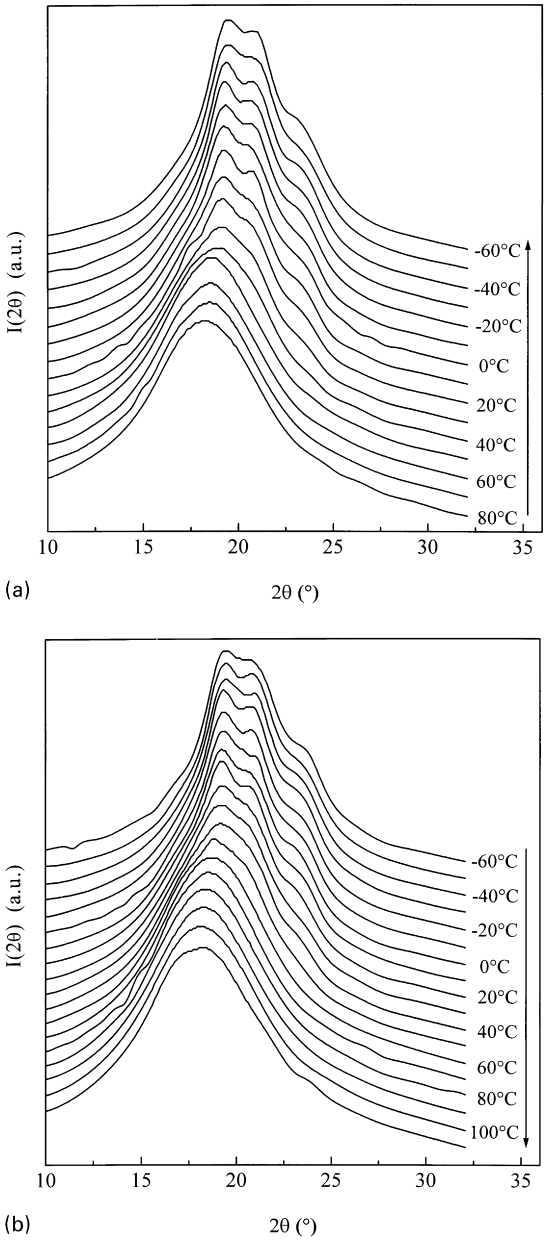

Fig. 6. WAXD-patterns of EO J during cooling from 150 to −60°C at −5°C/min (a) and subsequent heating at 10°C/min (b).

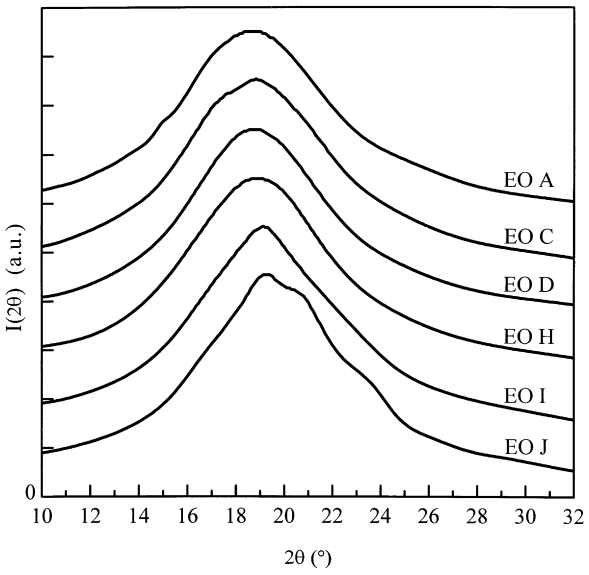

Fig. 7. WAXD-patterns at room temperature of homogeneous EO copolymers cooled at −5°C/min from 150 to −60°C and subsequent heated at 10°C/min. Successive patterns have been displaced by 3000 units along the ordinate for better visualisation.

At high temperatures the amorphous halo appears at lower angles, i.e. larger dimensions, due to thermal expansion effects, as already observed by McFaddin et al. [39]. In addition, like McFaddin et al. [39], it is found that with increasing 1-octene content at a constant temperature the amorphous halo of the EO copolymers shifts to lower angles.

Some authors [38–41] suggest that the sharpness of the *amorphous* halo is due to the superposition of an additional reflection on the halo of the liquid-like amorphous phase (as in the melt). Class et al. [38] assigned this additional peak to a fraction with order intermediate between crystalline and amorphous. Androsch et al. [41] assume that this additional reflection is due to a hexagonal mesophase.

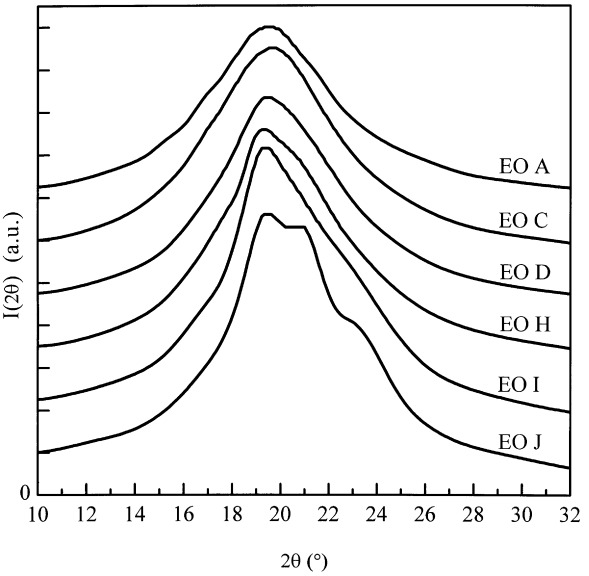

Fig. 8. WAXD-patterns at −60°C of homogeneous EO copolymers cooled from 150°C at −5°C/min. Successive patterns have been displaced by 2500 units along the ordinate for better visualisation.

The time-resolved WAXD intensities of EO J, during cooling from the melt to −60°C and subsequent heating, are shown in Fig. 6a and b respectively. During cooling weak orthorhombic 110- and 200-reflections appear around 30°C and disappear at approximately 40°C upon heating. These values should be compared with the on- and off-set temperatures of the SAXS-invariants and the crystallinities in DSC, which are approximately 45°C and 50°C respectively in cooling and 75°C and 80°C respectively in heating. Apparently, WAXD reflections are only observed above a certain threshold in the degree of crystallinity. As the comonomer content is further increased, leading to copolymer densities at room temperature below 870 kg/m^3, crystalline reflections are no longer observed at room temperature, as illustrated in Fig. 7, because the crystallites formed during crystallisation are too small and/or too imperfect. The same is observed at −60°C, as shown in Fig. 8, but asymmetric WAXD patterns, due to very weak underlying crystalline reflections, are still seen at room temperature densities between 855 and 870 kg/m^3 (EO I, EO H and EO D), indicating that these samples are not amorphous at −60°C. WAXD thus also suggests that below room temperature further growth and/or perfectioning of the crystallites occur during cooling.

Globally, the results of DSC, SAXS and WAXD indicate a continuous behaviour with increasing comonomer content. The thermal behaviour and the morphology change continuously, as already observed for the homogeneous EP and EB copolymers [17]. These observations, in combination with transmission electron micrographs [2], support a model in which with increasing branching content a gradual change of the morphology takes place from a lamellar base morphology into a granular one consisting of small, blocky structures. Further reduction of the crystallite dimensions could lead to a fringed-micelle morphology, although in absence of transmission electron microscopy (TEM) evidence this remains speculation. The reduction of the lateral dimensions of the lamellae to the same order of magnitude as of the longitudinal one, as is the case for the granular morphology, has different reasons. Firstly, the mobility of the chain segments is reduced because crystallisation occurs closer to the glass transition region. Secondly, the critical dimensions for a stable nucleus decrease due to the higher supercooling at higher branching contents. For the cooling rates used, these two features probably promote significant cocrystallisation of ethylene sequences of different lengths, leading to crystallites with a relatively low amount of re-entry of chains. The amount of chains that can leave a lamellar type crystal is however limited. Large numbers leaving chains cannot be dissipated effectively enough into the amorphous phase because such a situation is incompatible with the density of amorphous

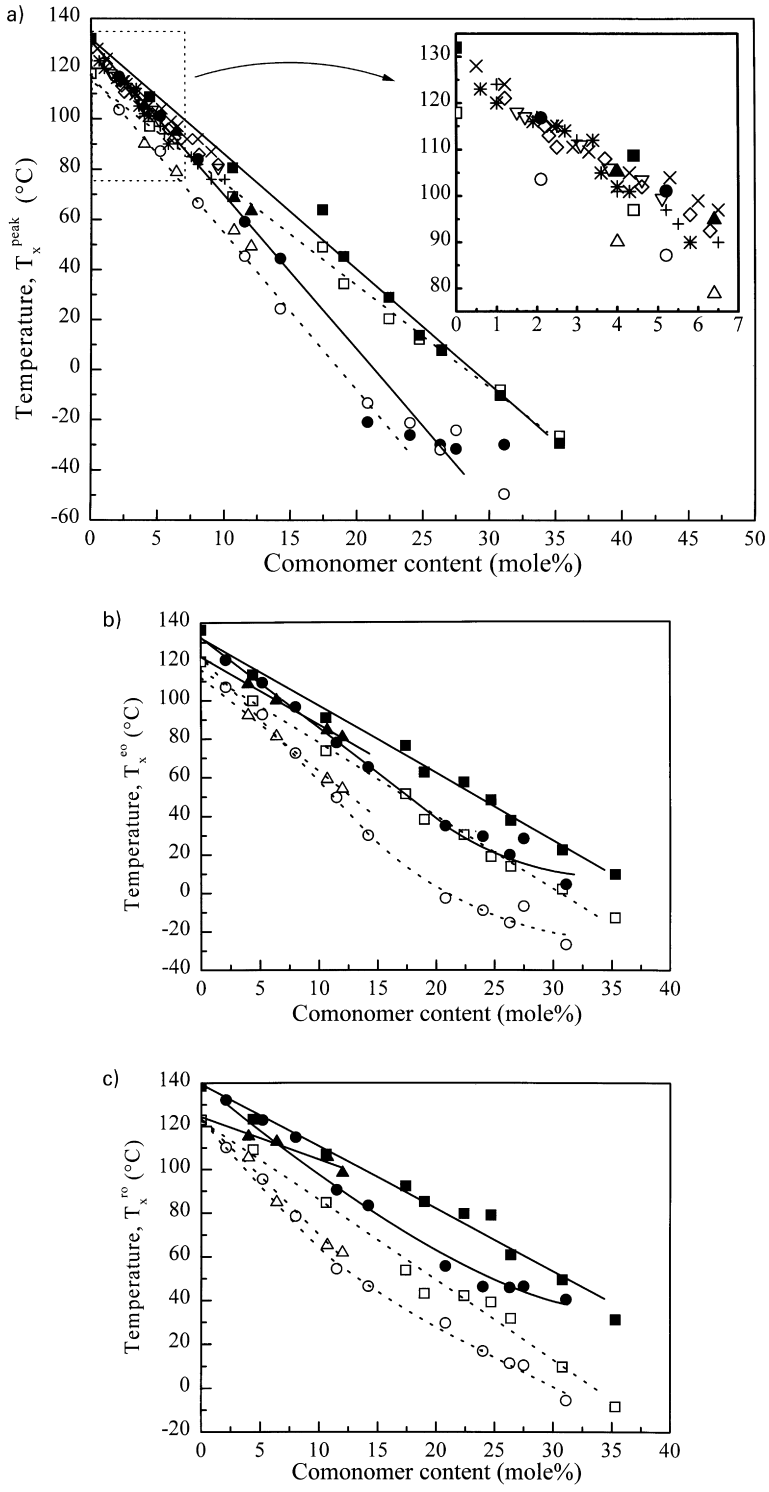

Fig. 9. Crystallisation (open symbols) and melting (solid symbols) temperatures of JW 1114 and homogeneous EP (squares), EB (triangles) and EO (circles) copolymers determined in three different ways: (a) peak temperature T_x^{peak}; (b) extrapolated on/offset temperature T_x^{eo}; (c) real on/offset temperature T_x^{ro}; T_m^{peak} of EB (×) and EO (+) copolymers after Clas et al. [18]; T_m^{peak} of EB (∗), EH (◇) and EO (▽) copolymers after Alamo et al. [30]. Lines are guides to the eye.

material. Such overcrowding effect [42,43] is cancelled by local curvature in the lamellae, by tilting of the chains in the crystal or—more effectively—by reduction of the lateral size of the crystallites.

In a certain range of comonomer content both morphologies (lamellae and granules) coexist [2], as was already observed by Minick et al. [44]. Apparently, there are copolymers whose comonomer distribution is such that the longest ethylene sequences are sufficiently long to fold into lamellae, while the shortest sequences can only form granular or

blocky structures, or even fringed-micelle crystallites. For copolymers with the highest comonomer contents, which crystallise just above the glass transition region, it is expected that only nearest-neighbour segments can crystallise [45], possibly resulting in *clusters of loosely packed ethylene sequences*. Such a morphology was suggested on the basis of Monte-Carlo simulations [2,46] but have, however, not yet been experimentally demonstrated.

3.2. Influence of comonomer type on thermal behaviour and morphology

The thermal behaviour and the morphology of homogeneous ethylene–1-alkene copolymers is also influenced by the comonomer type, since the branch length determines whether or not the short chain branch is inserted in the crystal. As already mentioned, methyl—and to a small extent also ethyl—branches can be incorporated in the crystal lattice, while the longer hexyl branches are completely excluded [9–11].

The influence of the comonomer type was already demonstrated for EP, EB and EO copolymers [17], although in the latter case only a single sample (EO J) was investigated.

As discussed previously [17], the influence of increasing branch length on the thermal behaviour is to some extent similar to that of increasing comonomer content: broader and flatter DSC-curves; shift of T_c, T_m and T_g to lower temperatures; and decreasing peak areas indicating lowering crystallinities.

Fig. 9 gives an overview of the crystallisation and melting temperatures as a function of comonomer content for the three different types of homogeneous ethylene–1-alkene copolymers (EP, EB and EO) and JW 1114, obtained by a vanadium-based catalyst except the EB copolymers which are made by use of a metallocene catalyst. T_c and T_m are defined as the peak temperature of the exo- and endotherm (T_x^{peak}), as the extrapolated on/offset temperature (T_x^{eo}) and as the real on/offset temperature (T_x^{ro}). The data (T_m^{peak}) obtained by Clas et al. [18] on EB and EO copolymers and by Alamo et al. [30] on EB, ethylene–1-hexene (EH) and EO copolymers are also given in Fig. 9a for comparison. It should be emphasised that the characteristic transition temperatures give only an impression of the temperature distributions as crystallisation and melting occur continuously over broad temperature regions.

Fig. 9 illustrates that, irrespectively of the determination method, the crystallisation and melting temperatures decrease more or less linearly with increasing comonomer content. Some deviation is observed in T_x^{peak} at high 1-octene contents, which results from the difficulty to accurately determine the position of the maximum in the very broad and flat DSC-curves at high comonomer contents. The lowering molar mass with increasing 1-octene content, might also partially cause the smaller decrease of T_c and T_m at high comonomer contents, as was also observed by Clas et al. [18]. They found also larger scatter in the melting peak temperatures of copolymers with higher 1-octene contents, which they ascribed partially to the large variation in molar masses (M_n from approximately 20–180 kg/mol). As in our case, they observe relatively high melting points in case of samples of low molar mass. So, even in case of highly branched copolymers, possibly, there is still an influence of molar mass [15,30].

Agreement is found with the results obtained by Class et al. [18] using a comparable catalyst system, as shown in Fig. 9a. The melting points reported by Alamo et al. [30] are somewhat lower, probably due to the rapid cooling before heating in their case.

In Fig. 10 the maximal crystallinities (w_{max}^c), i.e. the crystallinities just above the glass transition, of the different homogeneous ethylene–1-alkene copolymers and the LPE-sample are plotted as a function of comonomer content after cooling at −10°C/min from the melt. For all copolymers w_{max}^c decreases with increasing comonomer content. Again, the importance of temperature-dependent measurements is to be stressed; compare the results for w^c as shown here with those obtained at 23°C in Fig. 2. Below 10 mole% of comonomer, the measured w_{max}^c values do not differ systematically for different comonomer contents. At higher comonomer contents, however, the w_{max}^c-values are lower at higher branch lengths. Clearly, with increasing comonomer content, the crystallinities become zero (at different temperatures for propylene and 1-octene copolymers), either because the sequences are not capable anymore to crystallise and/or vitrification effectively interrupts crystallisation.

The fact that T_c, T_m and w_{max}^c decrease more rapidly with increasing comonomer content at higher branch length, is due to the ability of the methyl branches to be incorporated in the crystalline regions, while longer hexyl branches are excluded [9–11]. The bulkier the side chain, the more the building of large crystallites is hindered. For long branches a

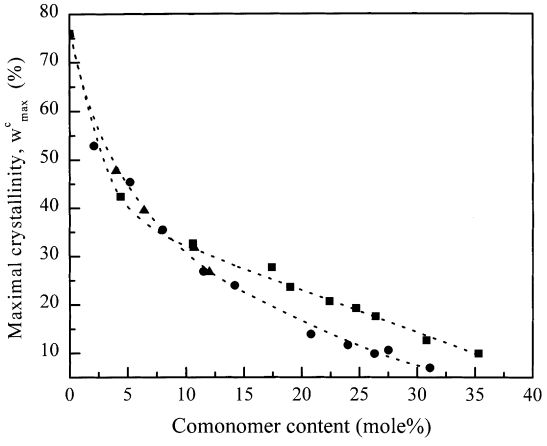

Fig. 10. Maximal crystallinity, w_{max}^c, as a function of the comonomer content of homogeneous EP (■), EB (▲) and EO(●) copolymers and JW 1114 after cooling at −10°C/min from the melt [17]. Lines are guides to the eye.

kind of dilution effect also plays a role: the mass fraction of the crystallisable ethylene sequences decreases as the branch length increases, resulting in a reduction of the amount of crystallisable material [18]. These DSC results are confirmed by the SAXS findings (see Fig. 4) and the WAXD findings, see before and [17], as follows from the ratio of the area of the crystalline peaks to the total area.

Finally, TEM micrographs of selected copolymers [2] reveal a morphology change with increasing branch length from a pure lamellar base morphology (EB 1, EB 2, EB 5) to a lamellar base morphology with also some granular structures present (EP 207) and via a granular base morphology with very few isolated lamellae (EO J) [2,17] to a granular base morphology (EP 203).

4. Conclusions

The influence of the comonomer content on the thermal behaviour and morphology of homogeneous ethylene–1-octene copolymers is qualitatively similar to that observed for homogeneous EP and EB copolymers [17]. With increasing comonomer content, the DSC cooling and heating curves become broader and flatter, while crystallisation and melting occur at lower temperatures approaching the glass transition. The latter becomes more pronounced and occurs at slightly lower temperatures. Further, the DSC-peak area decreases indicating lower crystallinities. Similar effects are observed with increasing side branch length when the heating curves of EP, EB and EO copolymers with the same comonomer contents are compared [17]. These observations reflect dimension distributions of increasingly small and/or imperfect crystalline structures with low thermal stability at higher comonomer contents or longer branch lengths.

This also explains the less pronounced crystalline orthorhombic 110- and 200-reflections in WAXD with increasing comonomer content. For EO copolymers with room temperature densities below 870 kg/m^3 no WAXD reflections are any longer observed at room temperature, indicating the presence of very small and/or too imperfect crystallites. At lower temperatures, down to −60°C, however, the WAXD patterns become asymmetrical for copolymers with room temperature densities of between 855 and 870 kg/m^3, due to very weak underlying crystalline reflections. Since this is not the case at room temperature, further growth and perfectioning of the crystallites must occur below room temperature.

For all copolymers a change in the SAXS-invariant is observed during cooling and heating. This means that, even in the copolymer with the highest comonomer content (44 mole% 1-octene)—which reveals no crystallisation-related peaks in DSC—structures with electron densities differing sufficiently from the amorphous surroundings are formed. All copolymers reveal a correlation maximum in the SAXS-curve after subtraction of a melt pattern, which indicates the periodic nature of these fluctuations.

When comparing homogeneous ethylene copolymers of different short chain branch lengths, all effects associated with increasing comonomer content appear to be stronger at higher side branch lengths. For instance, the crystallisation and melting temperatures decrease more sharply with increasing comonomer content at higher branch lengths, irrespective of the determination method. Also, the WAXD reflections disappear sooner in the case of EO copolymers with a higher degree of branching. Clearly, EO copolymers have lower densities and crystallinities than EP copolymers of the same comonomer contents. These observations confirm that methyl, and possibly ethyl, groups exercise a smaller hindrance on crystallisation by insertion in the crystal lattice, while the longer hexyl branches are rejected and, therefore, hinder crystallisation to a much larger extent, leading to smaller and less stable crystallites.

The different techniques reveal a continuous behaviour with increasing comonomer content. This supports a model which describes a gradual change with increasing comonomer content from a lamellar base morphology into a granular one consisting of small, imperfect, blocky structures, and, possibly via fringed-micelles, into a morphology consisting of loosely packed ethylene sequences.

Acknowledgements

This research was supported by the Research Council of the K.U.Leuven, the Fund for Scientific Research Flanders (F.W.O.-Vlaanderen) and DSM Research (Geleen). One of the authors (S.V.E.) is indebted to the Flemish Institute for the Promotion of Scientific and Technological Research in Industry (I.W.T.) for a fellowship. V.M.—on leave from DSM Research, Geleen, The Netherlands—is indebted to the K.U.Leuven for a guest professorship. We thank the European Union for support of the work at the EMBL Outstation in Hamburg under the TMR/LSF program (ERBFMGECT980134).

References

[1] Mathot VBF, Scherrenberg RL, Pijpers MFJ, Bras W. J Therm Anal 1996;46(3/4):681.
[2] Mathot VBF, Scherrenberg RL, Pijpers MFJ, Engelen YMT. In: Hosoda S, editor. The new trends in polyolefin science and technology, Publisher Research Signpost, 1996. p. 71.
[3] Mathot VBF. In: Mathot VBF, editor. Calorimetry and thermal analysis of polymers, New York: Hanser, 1994. p. 231 chap. 9.
[4] Mathot VBF, Scherrenberg RL, Pijpers MFJ. Polymer 1998;39(19):4541.
[5] Defoor F, Groeninckx G, Schouterden P, Van der Heijden B. Polymer 1992;33(18):5186.
[6] Reddy SS, Swaram S. Prog Polym Sci 1995;20(2):309.
[7] Bensason S, Minick J, Moet A, Chum S, Hiltner A, Baer E. J Polym Sci Polym Phys 1996;34:1301.

[8] Kravchenko R, Waymouth RM. Macromolecules 1998;31(1):1.
[9] Kortleve G, Tuijnman CA, Vonk CG. J Polym Sci Polym Chem 1972;10:123.
[10] Hosoda S, Nomura H, Gotoh Y, Kihara H. Polymer 1990;31:1999.
[11] Vonk CG, Reynaers H. Polym Commun 1990;31:190.
[12] Wunderlich B. Macromolecular physics, vol. 3: crystal melting, New York: Academic Press, 1980. p. 235 chap. 10.
[13] Vanden Eynde S. Master thesis. Katholieke Universiteit Leuven, Belgium, 1995.
[14] Peeters M, Goderis B, Vonk C, Reynaers H, Mathot V. J Polym Sci Polym Phys 1997;35:2689.
[15] Peeters M. PhD thesis. Katholieke University Leuven, Belgium, 1995.
[16] Goderis B, Reynaers H, Koch MHJ, Mathot VBF. J Polym Sci Polym Phys 1999;37:1715.
[17] Vanden Eynde S, Mathot VBF, Koch MHJ, Reynaers H. Submitted for publication.
[18] Clas S-D, McFaddin DC, Russell KE, Scammel-Bullock MV, Peat IR. J Polym Sci Polym Chem 1987;25:3105.
[19] Flynn JH. Thermochim Acta 1974;8:69.
[20] Moyhnihan CT, Esteal AJ, De Bolt MA, Tucker J. J Am Ceram Soc 1976;59:12.
[21] Richardson MJ, Savill NG. Br Polym J 1979;11:123.
[22] Mathot VBF, Pijpers MFJ. J Therm Anal 1983;28:349.
[23] Mathot VBF. In: Mathot VBF, editor. Calorimetry and thermal analysis of polymers, New York: Hanser, 1994. p. 105 chap. 5.
[24] Mathot VBF. Polymer 1984;25:579 Errata: Mathot VBF. Polymer 1986;27:969.
[25] Wunderlich B, Czornyj G. Macromolecules 1977;10(5):906.
[26] Koch MHJ, Bordas J. Nucl Instrum Methods 1983;208:435.
[27] Gabriel A. Rev Sci Instrum 1977;48:1303.
[28] Peeters M, Goderis B, Reynaers H, Mathot V. J Polym Sci Polym Phys 1999;37:83.
[29] Strobl GR, Schneider M. J Polym Sci Polym Phys 1980;18:1343.
[30] Alamo RG, Mandelkern L. In: Mathot VBF, editor. Thermal analysis and calorimetry in polymer physics, Special issue Thermochim Acta, 238. 1994. p. 155.
[31] Vanden Eynde S, Goderis B, Mathot VBF, Koch MHJ, Reynaers H. In preparation.
[32] Mathot VBF, Scherrenberg RL, Pijpers MFJ. Polymer 1998;39(19):4541.
[33] Goderis B, Mathot VBF, Reynaers H. Preprints ACS National meeting: semi-crystalline polymers, New Orleans, LA, 22–26 August 1999.
[34] Maurer JJ. Rubber Chem Technol 1965;38:979.
[35] Flory PJ. J Chem Phys 1947;15(9):684.
[36] Flory PJ. Trans Faraday Soc 1955;51:848.
[37] Kilian HG. In: Mathot VBF, editor. Thermal analysis and calorimetry in polymer physics, Special issue Thermochim Acta, 238. 1994. p. 113.
[38] Clas SD, Heyding RD, McFaddin DC, Russell KE, Scammel-Bullock MV. J Polym Sci Polym Phys 1988;26:1271.
[39] McFaddin DC, Russell KE, Wu G, Heyding RD. J Polym Sci Polym Phys 1993;31:175.
[40] Androsch R. Polymer 1999;40(10):2805.
[41] Androsch R, Blackwell J, Chvalun SN, Wunderlich B. Macromolecules 1999;32:3735.
[42] Flory PJ. J Am Chem Soc 1962;84:2857.
[43] Vonk CG. J Polym Sci Polym Lett 1986;24:305.
[44] Minick J, Moet A, Hiltner A, Baer E, Chum SP. J Appl Polym Sci 1995;58:1371.
[45] Wunderlich B. Macromolecular physics, vol. 2: crystal nucleation, growth, annealing, New York: Academic Press, 1976. p. 181 chap. 6.
[46] van Ruiten J, van Dieren F, Mathot VBF. In: Dosière M, editor. Crystallization of polymers, Dordrecht: Kluwer Academic, 1993. p. 481.